Research Square

Preprints are preliminary reports that have not undergone peer review.
They should not be considered conclusive, used to inform clinical practice,
or referenced by the media as validated information.

Selenium nanoparticles as slow-release fertilizers for mustard plants

Rewati Dixit
Indian Institute of Technology Delhi
Norbert Jordan
Helmholtz-Zentrum Dresden-Rossendorf e.V
Rohan Jain
r.jain@hzdr.de

Helmholtz-Zentrum Dresden-Rossendorf e.V, Helmholtz Institute Freiberg for Resource Technology

Research Article

Keywords: biogenic Se nanoparticles, plant growth, bio-nanofertilizer, slow-release, sustainability

Posted Date: October 5th, 2026

DOI: https://doi.org/10.21203/rs.3.rs-10859357/v1

License: This work is licensed under a Creative Commons Attribution 4.0 International License.
Read Full License

Additional Declarations: No competing interests reported.

Abstract

Selenium (Se) is a key micronutrient involved in several major metabolic pathways in humans, but its deficiency has become a major concern worldwide due to its heterogeneous distribution on the Earth's surface. Conventionally, Se oxyanions have been used for fertilization, nonetheless, they are toxic and inefficient due to huge leaching losses. Thus, there is a need for safe and effective fertilizers. Microorganisms convert toxic Se oxyanions into non-toxic Biogenic Se nanoparticles (BioSeNPs). BioSeNPs contain elemental Se encapsulated by proteins or extracellular polymeric substances, depending upon the microbial origin. This surface capping acts as a protective layer around Se, preventing its quick release from the core. Considering this property, BioSeNPs produced by *E. coli* and anaerobic granular sludge were investigated as a slow-release fertilizer for Indian mustard in this study. First, the fundamental properties of the nanoparticles were studied, followed by leaching of BioSeNPs in soil and plant uptake investigation. BioSeNPs produced by *E. coli* and anaerobic granular sludge were able to retain 96.7±1.2% and 91.7±2.1% Se, respectively, in the soil, whereas 63.6±1.1% and 86.3±1.9% Se from selenite and selenate were lost due to leaching. Further, 10 g•ha^{-1} Se from BioSeNPs was applied in the soil to analyse their uptake by the mustard plants. 24.1±2.2 % and 28.5±2.4 % Se were assimilated in the plants (total assimilation in roots and shoots) from BioSeNPs produced by anaerobic granular sludge and *E. coli*, respectively, in the first 8 weeks. Thus, BioSeNPs can provide sustained release of Se that is bioavailable.

1. Clinical Trial Registration

Not applicable.

1. Introduction

Selenium (Se) is an essential micronutrient. It has a narrow range of safe intake range between 40-400 µg day^{-1}, beyond which it can cause selenosis [1]. Nonetheless, it is a key micronutrient involved in reproduction, antioxidation, muscle function, and tumour prevention [2]. A Se deficiency can cause Keshan disease, myxedematous cretinism, and osteoarthropathy [3]. Approximately 500-1,100 million people worldwide are Se-deficient [4]. A 2021 study reported mean serum Se levels of 79.1±10.9 ng•mL^{-1} for healthy individuals in South India, indicating a spreading deficiency [5]. Although the recommended Se dietary intake is low (30-55 mg/day), it largely depends on the foods consumed [6]. Se fortification is possible in Se-deficient soils via external application.

Conventional Se fertilizers, primarily sodium selenite and sodium selenate salts [7], exhibit high water solubility, resulting in 70-90% Se loss through runoff and leaching [8–11]. This necessitates the development of slow-release Se fertilizer for efficient biofortification of food. Biogenic Se nanoparticles (BioSeNPs), consisting of elemental Se capped by biomolecules [12, 13], structurally resemble typical slow-release fertilizers, which slow the diffusion of the soil water to the fertilizer core [14]. Since BioSeNPs can be produced microbially by the reduction of selenite or selenate, they represent

sustainable candidates as a slow-release biofertilizer for overcoming Se deficiency. However, no such studies have ever been carried out.

BioSeNPs are predominantly produced as amorphous elemental Se core enveloped by proteins or extracellular polymeric substances (EPS), forming a sphere, with coating composition depending on their microbial origin [12]. For instance, *E. coli*-produced Se nanoparticles are protein-capped, whereas the ones produced by anaerobic granular sludge are coated with EPS [12, 13]. This outer coating governs the surface charge and colloidal stability of the nanoparticles [13, 15].Thus, the surface corona is important when studying BioSeNPs interaction with the environment. On one hand, the surface charge provided by the corona may create electrostatic repulsion, preventing aggregation and soil pore straining [16]. On the other hand, these nanoparticles could adhere to oppositely charged soil particles, thereby restricting their transport and mobility [16].However, such studies have not yet been carried out. The application of BioSeNPs as slow-release fertilizers has not been explored so far. The mobility and transport of BioSeNPs in soil and their uptake by plants, including mustard, remain understudied.

This study investigated the ability of BioSeNPs produced by pure and mixed microbial cultures to be used as a slow-release Se fertilizer. *E. coli* and anaerobic granular sludge from the pulp and paper industry have been used to synthesize BioSeNPs with different coatings. The BioSeNPs were characterized (shape, crystal nature, surface charge, and chemical composition of the coating), and their colloidal stability was studied. The BioSeNPs were then applied as slow-release Se fertilizer to study their release in soil and uptake of Se in the Indian mustard plant because it is a good Se accumulator, grows fast, produces significant biomass and Se metabolism is well characterized to provide a framework for uptake studies [7, 17].

2. Materials and methods

2.1. Materials

Luria-Bertani broth (Miller), sodium hydroxide pellets, concentrated hydrochloric acid, sodium selenite, sodium selenate, phenol, sulfuric acid, Folin and ciocalteu's phenol reagent (2N), and ferric chloride were purchased from Sigma Aldrich, whereas ammonium chloride, potassium dihydrogen phosphate, dipotassium hydrogen phosphate, magnesium chloride, calcium chloride dihydrate, yeast extract, and glucose were procured from Himedia. All chemicals were reagent grade with a purity of ≥99.5%. Wild-type *E. coli* K12 strain MG1655 (CGSC# 6300) was obtained from the *Escherichia coli* genetic stock center (CGSC), Yale University. Anaerobic granular sludge was procured from an active Upflow anaerobic sludge blanket (UASB) reactor in an industry near Delhi, India.

2.2. Production and purification of BioSeNPs

BioSeNPs were produced using *E. coli* and anaerobic granular sludge. *E. coli* was revived from glycerol stocks stored at − 80°C and cultured in Luria-Bertani broth (Miller). The primary culture was made by inoculating the bacteria in the media and incubating at 30°C for 24 hours at 120 rpm. 2.5% of this

primary culture was added to the nutrient media containing 2.5 mmol•L^{-1} sodium selenite. The culture was incubated for 4 days at 30°C and 120 rpm, as mentioned in Fischer et al., [12].

For Se nanoparticles production by anaerobic granular sludge, the sludge was cultured in a glucose medium composed of 10 g glucose, 0.34 g yeast extract, 0.84 g ammonium chloride, 0.136 g potassium dihydrogen phosphate, 0.23 g dipotassium hydrogen phosphate, 0.084 g magnesium chloride, 0.05 g ferric chloride, and 0.09 g calcium chloride dihydrate for 1 L media along with 2.5 mmol•L^{-1} sodium selenite. 10% inoculum was used, and the culture was incubated at 37°C for 7 days.

BioSeNPs were purified using the method described in Jain et al., [18]. Briefly, the culture was centrifuged at 37,000 *g* for 30 minutes at 4°C. The pellet was washed thrice with Milli-Q (18 MΩ·cm) and sonicated for 1 hour at 100 Watt and 42 kHz in ice. The pH of the solution was then raised to 12.5 using 1 N NaOH and further sonicated for 2 hours. Then, the pH was brought back to 7.3 by adding 1 N HCl. An equal volume of *n*-hexane was added to the solution in a separatory funnel and left undisturbed overnight. The BioSeNPs were then collected in the aqueous phase and washed three times with Milli-Q to remove any remaining *n*-hexane. The nanoparticles were then re-suspended in Milli-Q, and pH was re-adjusted to 7.3 with 1 N NaOH.

The alkaline treatment (pH 12.5) combined with prolonged sonication was intended to lyse residual microbial cells and substantially reduce biomass contamination, while *n*-hexane extraction removed remaining hydrophobic cellular debris [18, 19]. Jain et al. [18] showed that the purification process only removed the excess biomass, and the strongly bound biomolecular corona was retained, as shown by Energy-Dispersive X-ray Spectroscopy (EDX) and X-ray Photoelectron Spectroscopy, thereby maintaining the colloidal stability, as seen in the zeta potential of − 31.0 mV at pH 7 and a 5 mM NaCl background electrolyte.

2.3. Characterization of BioSeNPs

Scanning electron microscopy (SEM) was performed using a JEOL JSM-7800F FESEM at 50 kV and LN2 free SDD X-max 80 EDS detector to investigate the morphology of the nanoparticles. The aqueous suspension of BioSeNPs was dropped on a glass slide and dried overnight at 37°C. It was then coated with gold and viewed. EDX was also performed for BioSeNPs. ImageJ software was used to analyze the size of BioSeNPs. The size of at least 100 nanoparticles was measured and plotted in a histogram with the normalised curve to find the average particle size. Raman spectroscopy was performed using a Renishaw Micro Raman spectrometer to study the nature of the nanoparticles. The BioSeNPs aqueous suspension was centrifuged at 15,400 *g* and 4°C for 15 minutes. The supernatant was removed, and BioSeNPs were air-dried overnight. Then, the nanoparticles were mounted on an aluminium slide to be analysed by the spectroscope. Normal Raman spectra were acquired at 785 nm excitation and 5 mW for a spectral range of 150-2,100 cm^{-1}. An acquisition interval of 10 seconds was maintained, and all spectra were averaged over 10 independent runs.

Malvern Nano ZS zetasizer was used to study the zeta potential of the particles. 1 and 100 mmol•L^{-1} NaCl was added to the aqueous suspension of 10 mg•L^{-1} BioSeNPs as a background electrolyte, and each sample was titrated using 0.25, 0.025 mol•L^{-1} HCl and 0.25 mol•L^{-1} NaOH while measuring zeta potential from pH 9 to pH 2 with the help of MPT-2 titrator attached to the zetasizer. This led to the identification of the isoelectric point (pI) of the BioSeNPs. A liquid-filled glass combination electrode was used in an MPT-2 titrator for pH measurements. A two-point calibration was done for the electrode using Thermoscientific pH calibration buffers of pH values 4.01 and 10.01 at 25°C.

To study the colloidal stability of BioSeNPs, 20 mL solution of 10 mg•L^{-1} of BioSeNPs with an initial pH of 7.3 was gradually spiked with calcium chloride dihydrate to achieve the desired concentration in the range 0–20 mmol•L^{-1}. Then, the zeta potential of BioSeNPs was measured for all the conditions. The final pH was not controlled to prevent interference of the reaction between salt and BioSeNPs, as mentioned in Jain et al., [15].

Chemical composition of the surface corona of all BioSeNPs was also studied by means of biochemical assays. 10 mg•L^{-1} BioSeNPs were sonicated for 15 minutes at 23 kHz, followed by centrifugation at 37,000 *g* at 4°C for 30 minutes. The supernatant was collected and analysed for carbohydrates, proteins, and humic acid using the phenol-sulfuric acid method and modified Lowry's method, respectively [20, 21].

2.4. Settling of BioSeNPs

The settling efficiency of BioSeNPs was measured for seawater, acidic water, and freshwater. The various types of water were synthetically prepared as per the standard protocols from Kester et al., [22] and Smith et al., [23]. The water was filled in a 25 mL measuring cylinder, and 10 mg•L^{-1} BioSeNPs were added on top of the liquid to make up the volume to 25 mL. It was left undisturbed for 24 hours, after which samples were collected from 1 cm below the surface to analyse the suspended Se using Inductively Coupled Plasma Mass Spectrometry (ICP-MS) by dissolving them in concentrated HNO_3 [15]. H_2:He (7:93) was used as reaction gas, and ^{78}Se was used for quantification while ^{80}Se was used for verification. The samples were diluted 50-fold in 0.5% HNO_3 and were injected in a 1:1 ratio with the internal standards of Li, Ga, Sc, Rh and Ir. The entire system was flushed with ultrapure 0.5% HNO_3 in Milli-Q water.

2.5. Soil characterization

Soil was collected from the nursery in IIT Delhi at 28.545° latitude and 77.195° longitude from a depth of 15 cm. It was air-dried overnight at 37°C and filtered through a 2 mm sieve. The soil was mixed with a 0.01 mol•L^{-1} $CaCl_2$•$2H_2O$ solution at a 1:20 (w/v) soil-solution ratio, and pH was measured using a Cyberscan 510 pH meter with a double-junction combined pH electrode [24]. The calibration process of the electrode was the same as mentioned above. Electrical conductivity was measured using an Aquaread Aquameter, a multi-parameter water quality meter. The moisture content was measured by

calculating the weight loss after placing a crucible containing 100 g of soil in a Tanco Temperature Controller muffle furnace at 105°C for 24 hours. Organic matter and organic carbon were measured by weighing 10 g of soil in a crucible and placing it in the muffle furnace at 105°C for 4 hours [25]. The soil weight was taken after cooling down and noted as W1. Then, the crucible containing the soil was placed again in the muffle furnace at 400°C for 4 hours. It was then weighed as W2. The organic carbon and organic matter were calculated as given in equations 1 and 2. The second equation is based on the van Bemmelen conversion factor, which assumes that soil organic matter contains 58% carbon [26].

$$\%\, organic\, matter = \frac{W1-W2}{W1} \times 100 \text{ (Eq. 1)}$$

$$\%\, organic\, carbon = \%\, organic\, matter \times 0.58 \text{ (Eq. 2)}$$

Soil bulk density was calculated by measuring the weight and volume of soil that could fill a 500 mL beaker [27]. To measure particle density, 40 g of soil was placed in a 100 mL measuring cylinder. 50 mL of water was added and stirred, followed by the addition of 10 mL more water. The suspension was allowed to settle for 5 minutes, and the volume of soil was recorded. The soil bulk density and particle density were calculated as given in equations 3 and 4, respectively.

$$Bulk\ density\ \left(\frac{g}{cc}\right) = \frac{weight\ of\ soil\ (g)}{Volume\ of\ soil\ (cc)} \text{ (Eq. 3)}$$

$$Particle\ density\ \left(\frac{g}{cc}\right) = \frac{weight\ of\ the\ soil\ (g)}{volume\ recorded\ (cc)} \text{ (Eq. 4)}$$

A sample of the prepared soil was digested with aqua regia in a closed vessel microwave digestion system to prevent volatilization of Se and analyzed by ICP-MS to measure Se content in soil.

2.6. Se release

2 kg of soil, as prepared above, was packed in 15 pots with collection plates. 10 g•ha^{-1} Se from sodium selenite, sodium selenate, BioSeNPs produced by *E. coli* and anaerobic granular sludge (as measured from ICP-MS, which implies that the selenium concentration applied in the soil is same for all fertilizers) were added to three pots each and mixed homogeneously, whereas the remaining three pots did not contain added Se (negative control). These pots were maintained at 27–30°C and 12 hours of light. Keeping in mind 400 mm of water required for Indian mustard (later used as a model plant for uptake studies), the soil was watered, and leachate was collected from the bottom in the pot plates. This experiment lasted 56 days. The samples were dissolved completely in concentrated HNO_3 to convert elemental selenium to ionic selenium[28]. It was then diluted 1,000 times using Milli-Q. Further, the diluted samples were filtered using a 0.2-micron nylon syringe filter and the first 1 mL filtrate was discarded to saturate active sites and prevent any sorption losses. Additionally, Dalai and Biswas[29] showed that nylon syringe filter does not interact with ionic selenium. Hence, Se wouldn't be lost during filtration of the sample for ICP-MS analysis. The total Se was then analysed using ICP-MS, as previously described.

2.7. Se uptake by plants

The seeds for Indian mustard were procured from a local nursery and grown to a four-leaf stage in cocopeat under 12 hours of light and 30°C temperature conditions. These saplings were then transferred to pots with 2 kg of soil, which was prepared as mentioned above. Se was added at 10 g•ha^{-1} concentration in triplicate in the form of sodium selenite, sodium selenate, and freshly prepared BioSeNPs produced by *E. coli*, and anaerobic granular sludge. The Se concentration for each fertilizer was measured by ICP-MS, and it was maintained at 10 g•ha^{-1} for all fertilizer types. Three pots did not receive any additional Se fertilizer. No other fertilizer was added to the soil. The plants received 12 hours of light and water as per the 400 mm annual requirement of mustard. A temperature of 27–30°C was maintained. 100 mL of water was added to each pot once a week, and leachate was collected. The leachate was analysed for Se content as mentioned in the previous section. The plants and soil from pots were harvested after 56 days, during the flowering stage of the mustard plant. The length of roots and shoots was measured for all plants. The soil, plant roots, and shoots were dried, digested and analysed by ICP-MS for total Se content as mentioned above. Mass balance and Se distribution were calculated.

3. Results

3.1. Production and characterization of BioSeNPs

The BioSeNPs were successfully produced by *E. coli* and anaerobic granular sludge. BioSeNPs were harvested from the *E. coli* culture and anaerobic granular sludge cultured in a serum bottle after 4 and 7 days, respectively. The overall yield of the production and purification process of BioSeNPs by *E. coli* and anaerobic granular sludge is 93.8 ± 1.7% and 91.2 ± 2.0%, respectively. Elemental selenium exhibits Raman-active Se–Se vibrational modes whose positions depend on its allotrope. Trigonal selenium typically displays a stretching mode at ~ 235–238 cm^{-1}, whereas amorphous selenium exhibits a broad band centred around 250–255 cm^{-1} [30]. Raman spectra of the BioSeNPs showed a peak at 254 cm^{-1}, which is attributed to amorphous Se (Fig. 1a and b) [12, 15]. This evidently indicates the presence of elemental Se. The SEM images showed spherical nanoparticles irrespective of the microorganisms used to produce them (Fig. 1c and d). However, BioSeNPs produced by *E. coli* have an average particle size of 137 nm, whereas BioSeNPs produced by anaerobic granular sludge show an average particle size of 413 nm, as shown in Figs S1 (a) and (b) in the supporting information, respectively. The EDX of BioSeNPs revealed the presence of Se, O, C, S and N (Figs S2 and S3 in SI). The O, C, S, and N are attributable to the biomolecular corona of the BioSeNPs [31].

The BioSeNPs are negatively charged as per the zeta potential at neutral pH, as shown in Fig. 2(a), indicating the presence of a surface capping providing the surface charge. The zeta potential of BioSeNPs produced by E. coli and anaerobic granular sludge at pH 7.0 and 1 mM NaCl is − 34.6 ± 1.3 and − 25.3 ± 1.4 mV, respectively. However, the zeta potential decreases as the pH increases from pH 2 to 9.

The pI values of BioSeNPs produced by *E. coli* and anaerobic granular sludge at 1 mmol•L^{-1} NaCl background electrolyte were 2.9±0.1 and 2.8±0.1, respectively; whereas at 100 mmol•L^{-1} were 2.7±0.1, and 2.3 ± 0.1, respectively.

The colloidal stability, as represented by decreasing negative zeta potential, can be seen in Fig. 2(b). A major decline is observed in both BioSeNPs when calcium chloride is added at concentrations between 0 and 0.2 mmol•L^{-1}. However, the zeta potential trend is similar for both the BioSeNPs and the difference in the colloidal stability is minor. As shown in Fig. 2(c), both BioSeNPs show similar settling efficiency greater than 92% in seawater, acidic water, and freshwater. Thus, both BioSeNPs show similar properties.

The investigation of surface corona revealed that the BioSeNPs produced by pure cultures are primarily composed of proteins, whereas the BioSeNPs produced by anaerobic granular sludge have both carbohydrates and proteins as major components. The composition for each BioSeNPs is given in Table 1. The surface capping composition of *E. coli*-produced BioSeNPs is in line with the BioSeNPs produced by Xu et al. [32] using *Comamonas testosteroni* S44, where protein and carbohydrates were reported to be 1069 and 23 mg•g^{-1}.

Table 1
Surface corona composition of BioSeNPs

Components	**Carbohydrate (mg•g^{-1} of BioSeNPs)**	**Protein (mg•g^{-1} of BioSeNPs)**	**Humic acid (mg•g^{-1} of BioSeNPs)**
BioSeNPs from *E. coli*	4.7 ± 3.4	934.5 ± 90.8	27.5 ± 8.9
BioSeNPs from Anaerobic granular sludge	115.8 ± 24.2	287.4 ± 41.7	26.1 ± 10.0

3.2. Soil characteristics and Se release kinetics

The pH of the soil was measured to be 7.1 ± 0.1, and the conductivity was noted as 2.4 ± 0.3 mS•cm^{-1}. The soil had a moisture of 16.1 ± 0.2%. The organic matter in soil was recorded as 1.2 ± 0.1% while organic carbon was 0.7 ± 0.2%. The soil bulk density was calculated as 1.5 ± 0.3 g•$cm^{-3,}$ and the particle density was 2.5 ± 0.5 g•cm^{-3}. No Se was detected in the soil that was used for the Se release and uptake experiments. Once the soil parameters were established, the release of Se nanoparticles was studied. By 8 weeks (56 days), 63.6±1.1% and 86.3±1.9% Se was lost, respectively, from the soil when sodium selenite and sodium selenate were added to the pots without plants to study the release (Fig. 3). However, only 3.4 ± 2.4% and 9.6 ± 3.6% of the Se had leached from the soil by 8 weeks after application as nanoparticles produced by *E. coli* and anaerobic granular sludge, respectively, as shown in Fig. 3. Hence, BioSeNPs show better retention in soil than Se oxyanions (Fig. 4). Complete mass balance for the same is given in Table S1 in SI.

3.3. Se uptake by plants

After 8 weeks of growth, the root and shoot lengths of the plants were measured. In the absence of Se, the root length was merely 9 ± 0.6 cm, whereas in the presence of Se, it was 12 ± 0.6 cm for selenite and 13 ± 0.7 cm for the rest. Minimum shoot length was observed at 19 ± 1.0 cm for the control setup, whereas the maximum shoot length of 58 ± 2.7 cm was observed for the plant whose soil was fertilized with sodium selenate. The comparison of the morphological features of the plants fertilized by BioSeNPs is shown in Fig. 5.

When studying the Se distribution in plants in Fig. 6, it is interesting to note that, irrespective of the type of Se fertilizer used, roots absorbed only 11% of the Se provided by the soil till 8 weeks. Further, most of the Se absorbed was accumulated in the shoots of the plants.

The shoot Se content in plants fertilized with selenite, selenate, BioSeNPs produced by *E. coli* and anaerobic granular sludge is 7.5 ± 1.1%, 15.7 ± 2.3%, 17.3 ± 2.1% and 13.0 ± 2.2%, respectively (Fig. 6), of the initial Se added in soil. It should be noted that maximum Se has been absorbed in the shoot of plants fertilised by BioSeNPs produced from *E. coli*. Refer to Table S2 in SI for complete mass balance.

4. Discussion

4.1. BioSeNPs as slow-release fertilizers for Se fortification of mustard plant

This study demonstrated for the first time that BioSeNPs can be utilised as slow-release fertilizers in soil for Se fortification. BioSeNPs showed better retention in soil when compared to Se oxyanions (Fig. 4). 63.6 ± 1.1% and 86.3 ± 1.9% selenite and selenate leached off, respectively, from the soil in 8 weeks. However, 96.7 ± 1.2% and 91.7 ± 2.1%, Se was retained in soil for BioSeNPs produced by *E. coli* and anaerobic granular sludge, respectively. This can be attributed to the surface corona of the BioSeNPs, which lilkely slows the Se release from its core in comparison to the oxyanions, which are highly water-soluble. To exemplify, it has been shown that silver nanomaterials capped with sulfidated Polyvinylpyrrolidone (PVP) reduced the rate of silver ion release in solution and oxidation of the iron oxide core was prevented by their polyvinyl alcohol coating [33]. Moreover, citrate, branched polyethyleneimine, and thiolated hydrocarbon chains hinder reactions with the surrounding medium, such as oxidation and dissolution, when capped on silver nanomaterials [34–36]. Hence, surface coating acts as a barrier against interaction with the immediate environment and allows for a gradual release. To our knowledge, this is the first work to discuss the role of surface coating in the release of Se from the core in soil.

Similarly, in the presence of plants, BioSeNPs were more retained compared to the sodium Se salts. In comparison to selenite, BioSeNPs produced by *E. coli* and anaerobic granular sludge showed 87.7% and 78.3% less leaching (Fig. 3), respectively. Again, in the presence of plants, BioSeNPs from anaerobic

granular sludge and *E. coli* showed 3.3- and 3.5-fold better soil retention than selenate (Fig. 6). All these can be attributed to the surface coating present on the BioSeNPs.

Se assimilation by plants fertilized by BioSeNPs from anaerobic granular sludge and *E. coli* was 26.8% and 50.0% better, respectively, than selenite. Also, BioSeNPs produced 8% longer roots than selenite in mustard plants. This can be linked to the slow uptake of selenite due to passive absorption by plant roots [37]. Furthermore, compared with selenite, BioSeNPs produced by *E. coli* and anaerobic granular sludge yielded 80.0% and 29.2% taller plants, respectively, because selenite tends to accumulate mostly in the root system, resulting in poor shoot growth due to a lack of Se [38]. Thus, selenite gives lesser Se uptake in comparison to BioSeNPs [38]. Indeed, for instance, BioSeNPs produced by *E. coli* and anaerobic granular sludge produced approximately 2.4 and 1.7 fold taller plants, respectively, than the control setup where no fertilizer was applied (Fig. 5).

When comparing selenate and BioSeNPs, it was observed that the Se uptake in plants was comparable for all of them. In fact, selenate could be absorbed 9% more effectively than BioSeNPs from anaerobic granular sludge (Fig. 6). This can be attributed to the rapid and easy uptake of selenate via sulfate transporters in the roots. The selenate-fertilized plants showed the maximum shoot length of 58.0 ± 2.7 cm in contrast to the shoot length of 45.0±3.6 cm and 32.3±1.5 cm for BioSeNPs from *E. Coli* and from anaerobic granular sludge, respectively. The reason is that selenate is easily translocated through the xylem from the roots to the shoot, where it gets assimilated into organic Se [39]. Approximately 70–90% of the selenate taken up by plant roots in wheat is translocated to the shoot within 24 hours [37]. This perturbs the reductive sulfur assimilation pathway, which causes accumulation of signalling intermediate O-acetylserine, mimicking functional sulfur deficiency. It leads to a slight elevation of tryptophan levels in the cells, which is an important precursor for Auxin, a hormone responsible for shoot elongation [38]. Even a subtle increase in auxin leads to cascading effects such as up-regulation of Gibberellins biosynthesis, providing instruction for expansion [38]. Hence, it may induce a physiological response of shoot elongation and plant lengthening.

Nonetheless, BioSeNPs produced by *E. coli* could be absorbed 7.5% more than selenate. This is possible because nanomaterials can use alternate pathways from the sulfate transport system, like aquaporin-mediated fluidic phase entry. Studies have shown that approximately 60% Se nanomaterial influx is reduced if the aquaporin network is blocked [40]. Moreover, nanoparticles can also utilize active endocytosis, where the plasma membrane engulfs them into the interior or enter via the physical disruptions in the endodermis [41]. Further, the surface capping increases their biological affinity towards the root system and provides a negative surface charge (Fig. 2), which facilitates easier transport through lipid layers [40, 42]. Hence, BioSeNPs can be retained for a longer duration in soil and be taken up as easily as selenate, which is a frequently used fertilization option in fields.

Comparing the BioSeNPs, it can be seen that BioSeNPs produced by *E. coli* resulted in taller plants as compared to BioSeNPs from anaerobic granular sludge. This may be attributed to better uptake of BioSeNPs from *E. coli* as mentioned previously. Further, as shown in Fig S1, the size of BioSeNPs

produced by anaerobic granular sludge is 3 times higher than that of BioSeNPs produced by *E. coli*, which would result in lower uptake by plant roots [43]. The lower particle size implies higher surface-to-volume ratio, which enhances its reactivity and the probability of navigating through the porous matrix of the plant cell wall [44]. Hence, the probability of lower particle size nanoparticles entering the plant roots is higher. Moreover, the difference in the surface capping of the nanoparticles also influences the translocation of nanoparticles in plants. It has been shown that algal polysaccharide-capped chemically synthesized Se nanoparticles (CheSeNPs) when applied to the roots of rice plants in a hydroponic setup, exhibit a very low translocation factor and accumulate in the roots [42]. As seen from Table 1, BioSeNPs from *E. coli* are covered by proteins, whereas BioSeNPs from anaerobic granular sludge are covered by extracellular polymeric substances, which contain proteins and carbohydrates. Therefore, it is possible that due to the presence of carbohydrate in the surface corona of BioSeNPs from anaerobic granular sludge, their translocation to the shoot is comparatively lesser, which can be seen as lower shoot length in the plant.

Further, approximately 11% Se is absorbed in all plants' roots irrespective of the fertilizer type, and the rest is present in the shoot tissues. In general, it has been reported in the literature that Se tends to deposit in the shoot of the Se hyperaccumulators [45]. Indian mustard and sunflower when fertilized with 1 $mg \bullet L^{-1}$ selenate, assimilate more than half of the Se taken up by roots in the shoots [46]. *Astragalus bisulcatus* and *Stanleya pinnata* were reported to accumulate 4.8 and 2.7-fold Se in the shoot tissues on the treatment of 30 mg selenate per kg soil [47]. This is possible because hyperaccumulators can distinguish between sulfur and Se and preferentially take up Se, leading to higher Se:S ratios. This is attributed to elevated levels of S/Se transporters (SULTR) with greater specificity to Se. Moreover, high levels of Se are mitigated in hyperaccumulators by quickly converting them to highly mobile and detoxified organic Se, such as MeSeCys, which is translocated to the shoot via the xylem. It is then remobilised from older leaves to newer leaves via the phloem. High Se toxicity is prevented in their leaves by sequestering it in the vacuoles or edges of the leaves [45].

4.2. BioSeNPs vs conventional Se fertilizers

In general, the primary chemical forms of Se and some commercial formulation of Se are used as fertilizers in large-scale fields. Sodium selenate is preferred over sodium selenite in field application because selenite shows a low uptake rate by the plants [48]. However, it is known that the leaching losses for inorganic Se are high, and only 10–12% Se is taken up by non-Se-accumulator plants [49]. This is in corroboration with the findings in this study, as shown in Figs. 3 and 6, where approximately 60–80% Se oxyanions are lost in the leachate. Although the uptake was better because mustard is a Se accumulator. Moreover, these forms are toxic in nature, and microdosing is possible in fields since only 10 $g \bullet ha^{-1}$ Se needs to be added. Other than the chemical forms, certain specialized blends and carrier-based fertilizers are also commercially available. These involve the addition of 10 $g \bullet ha^{-1}$ Se in carriers like urea, di-ammonium phosphate or ammonium nitrate to ensure uniform dosing in large fields. Nonetheless, the presence of other ions like sulfate and phosphate hinders Se uptake due to competition. Hence, it reduces Se absorption efficiency. These bottlenecks can be taken care if Se

nanoparticles are added to the soil instead. These are comparatively less toxic, giving a high safety margin for application. They have enhanced penetration and uptake due to their small size and corona. Moreover, as discussed above, the leachability is significantly less, making it available for a longer duration of time and preventing frequent reapplication.

CheSeNPs coated with polyvinylpyrrolidone C15 also demonstrated that the pre-soaked barley seeds produced plants with two-fold root length when compared to unfertilized plants [50]. Likewise, wheat and rice plants consistently showed root elongation on application of CheSeNPs via the soaking method or foliar application [51, 52]. However, CheSeNPs require high-purity precursors and specialized equipment for production [53]. The manufacturing process for BioSeNPs is green and the cost would be less as it could be produced by ubiquitous microorganisms inoculated in Se-rich wastewater like flue gas desulfurization wastewater from power plants, desalter wash water from petroleum refinery, Se-laden wastewater from glass, electronics or metallurgical industries or media. In contrast to CheSeNPs which require additional coating to stabilize them, BioSeNPs are inherently coated with biomolecules providing them with colloidal stability essential for their transport, mobility, and interaction in soil. Furthermore, CheSeNPs coated with Bovine Serum Albumin (BSA) proved to be 10 times more toxic to zebrafish than BioSeNPs produced by anaerobic granular sludge [54].

4.3. Environmental relevance

This study evidenced the application of BioSeNPs as slow-release fertilizers for the first time. It showed that less than 10% Se was leached out from the soil containing BioSeNPs as fertilizers over the period of 8 weeks in comparison to selenite and selenate, which showed a loss of 63.6 ± 1.1% and 86.3 ± 1.9% Se, respectively. This agricultural runoff is detrimental to the ecosystem. The agricultural drainage of Se-laden water (500 $\mu g \bullet L^{-1}$) in the Kesterson Reservoir of the San Joaquin Valley of California caused deaths and deformities of fish and aquatic bird species [55, 56]. Further, the adult insect population around such water reservoirs in Prairie Pothole Regions of the USA and Canada was reduced by half, diminishing the food supply of terrestrial predators [57]. Additionally, the larvae retained Se in their tissues even after metamorphosis, which could lead to export of this Se further down the food chain of riparian consumers like spiders and birds [57]. Thus, BioSeNPs can help reduce Se pollution in agricultural runoff by limiting leaching losses. Moreover, approximately 24–28% of Se applied in soil in the form of BioSeNPs was taken up by the Indian mustard plant in 8 weeks and showed both shoot and root elongation in the plant, as shown in Fig. 5. Thus, BioSeNPs provide essential agricultural advantages over inorganic Se and have been shown to exert low disturbance to the microbial ecology and could promote the growth of important probiotics [58].

Declarations

Supporting Information

Extra figures showing the histograms for the average particle size of BioSeNPs, mass balance tables, and SEM-EDX figures of BioSeNPs as noted in the text (DOC).

Author Contributions

Rewati Dixit: Investigation, Methodology, Data Curation, Writing-original draft; Norbert Jordan: Writing-Review and Editing; Rohan Jain: Supervision, Writing-Review and Editing.

Funding

This work was supported by Prime Minister's Research Fellowship (PMRF), Ministry of Education, Government of India (PMRF ID: 1400791) awarded to Rewati Dixit.

Ethics and consent to participate

The Indian mustard seeds used in this study were purchased from a commercial local nursery in New Delhi, India. Plant cultivation was conducted in the nursery at the Indian Institute of Technology (IIT) Delhi, India. The acquisition and experimental handling of the plant material strictly complied with institutional, local, and national guidelines of India. No wild plant species were collected, and no special permissions or licenses were required for the commercial purchase and cultivation of this plant material.

Clinical Trial Registration

Not applicable.

Consent for publication

Not applicable.

Competing interests

The authors declare no competing interests.

Data availability

The data generated and analyzed in this study are included in the main manuscript and the supporting information.

References

1. Wen H, Carignan J (2007) Reviews on atmospheric selenium: Emissions, speciation and fate. Atmos Environ 41:7151–7165
2. Mehdi Y, Hornick JL, Istasse L, Dufrasne I (2013) Selenium in the environment, metabolism and involvement in body functions. Molecules 18:3292–3311
3. Vinceti M, Filippini T, Wise LA (2018) Environmental Selenium and Human Health: an Update. Curr environ health rep 5:464–485

4. White PJ, Broadley MR, Gregory PJ (2012) Managing the nutrition of plants and people. Appl Environ Soil Sci 2012:11–13. https://doi.org/10.1155/2012/104826
5. Muhammed M et al (2021) An exploratory study of selenium status in healthy individuals and in patients with COVID-19 in a south Indian population: The case for adequate selenium status. Nutrition 82:111053
6. Winkel LHE, Johnson CA, Lenz M et al (2012) Environmental selenium research: From microscopic processes to global understanding. Environ Sci Technol 46:571–579. https://doi.org/10.1021/es203434d
7. Golubkina N, Kekina H, Caruso G (2018) Yield, quality and antioxidant properties of indian mustard (Brassica juncea L.) in response to foliar biofortification with selenium and iodine. Plants 7. https://doi.org/10.3390/plants7040080
8. Schulz-Vogt HN, Pollehne F, Jürgens K et al (2019) Effect of large magnetotactic bacteria with polyphosphate inclusions on the phosphate profile of the suboxic zone in the Black Sea. ISME J 13:1198–1208. https://doi.org/10.1038/s41396-018-0315-6
9. Mast MA, Mills TJ, Paschke SS et al (2014) Mobilization of selenium from the Mancos Shale and associated soils in the lower Uncompahgre River Basin, Colorado. Appl Geochem 48:16–27. https://doi.org/10.1016/j.apgeochem.2014.06.024
10. Jones CP, Grossl PR, Amacher MC et al (2017) Selenium and salt mobilization in wetland and arid upland soils of Pariette Draw, Utah (USA). Geoderma 305:363–373. https://doi.org/10.1016/j.geoderma.2017.06.028
11. Xiang A, Li Y, Liu K et al (2024) Layered double hydroxide for slowing selenium fertilizer release and improving selenium utilization efficiency in vegetables. Appl Clay Sci 252. https://doi.org/10.1016/j.clay.2024.107340
12. Fischer S, Jain R, Krause T et al (2021) Impact of the Microbial Origin and Active Microenvironment on the Shape of Biogenic Elemental Selenium Nanomaterials. Environ Sci Technol. https://doi.org/10.1021/acs.est.0c07217
13. Jain R, Jordan N, Weiss S et al (2015) Extracellular polymeric substances govern the surface charge of biogenic elemental selenium nanoparticles. Environ Sci Technol 49:1713–1720. https://doi.org/10.1021/es5043063
14. Fu J, Wang C, Chen X et al (2018) Classification research and types of slow controlled release fertilizers (SRFs) used - a review. Commun Soil Sci Plant Anal 49:2219–2230. https://doi.org/10.1080/00103624.2018.1499757
15. Jain R, Jordan N, Tsushima S et al (2017) Shape change of biogenic elemental selenium nanomaterials from nanospheres to nanorods decreases their colloidal stability. Environ Sci Nano 4:1054–1063. https://doi.org/10.1039/c7en00145b
16. Tourinho PS, van Gestel CAM, Lofts S et al (2012) Metal-based nanoparticles in soil: Fate, behavior, and effects on soil invertebrates. Environ Toxicol Chem 31:1679–1692

17. Ogra Y, Ogihara Y, Anan Y (2017) Comparison of the metabolism of inorganic and organic selenium species between two selenium accumulator plants, garlic and Indian mustard. Metallomics 9:61–68. https://doi.org/10.1039/c6mt00128a
18. Jain R, Jordan N, Schild D et al (2015) Adsorption of zinc by biogenic elemental selenium nanoparticles. Chem Eng J 260:855–863. https://doi.org/10.1016/j.cej.2014.09.057
19. Dobias J, Suvorova EI, Bernier-Latmani R (2011) Role of proteins in controlling selenium nanoparticle size. Nanotechnology 22. https://doi.org/10.1088/0957-4484/22/19/195605
20. Dubois M, Gilles KA, Hamilton JK et al (1956) Colorimetric Method for Determination of Sugars and Related Substances. Anal Chem 28:350–356. https://doi.org/10.1021/ac60111a017
21. FrØlund B, Griebe T, Nielsen PH (1995) Enzymatic activity in the activated-sludge floc matrix. Appl Microbiol Biotechnol 43:755–761. https://doi.org/10.1007/BF00164784
22. Kester DR, Duedall IW, Connors DN, Pytkowicz RM (1967) Preparation of artificial seawater. Limnol Oceanogr 12:176–179
23. Smith EJ, Davison W, Hamilton-Taylor J (2002) Methods for preparing synthetic freshwaters. Water Res 36:1286–1296. https://doi.org/10.1016/S0043-1354(01)00341-4
24. Richards LA (1954) Diagnosis and improvement of saline and alkali soils. US Government Printing Office
25. Davras BE (1974) Loss-on-ignition as an estimate of soil organic matter 1. Soil Sci Soc Amer Proc 38
26. Pribyl DW (2010) A critical review of the conventional SOC to SOM conversion factor. Geoderma 156:75–83
27. Daddow RL (1983) Growth-limiting soil bulk densities as influenced by soil texture. Watershed Systems Development Group, USDA Forest Service
28. Constantinescu-Aruxandei D, Frîncu RM, Capră L, Oancea F (2018) Selenium analysis and speciation in dietary supplements based on next-generation selenium ingredients. Nutrients 10
29. Dalai S, Biswas A (2025) Colloidal association of selenite and selenate in water containing dissolved organic matter and ferric iron: implication for selenium mobility in the aquatic environments. Geochim Cosmochim Acta 399:156–170. https://doi.org/10.1016/j.gca.2025.04.027
30. Qamar N, Poimala M, Jäntti J et al (2026) Selenium nanoparticles as antioxidants: green synthesis, characterization, and evaluation of bioactivity. Biomater Sci 14:2317–2333. https://doi.org/10.1039/d5bm01855b
31. Buchs B, Evangelou MWH, Winkel LHE, Lenz M (2013) Colloidal properties of nanoparticular biogenic selenium govern environmental fate and bioremediation effectiveness. Environ Sci Technol 47:2401–2407. https://doi.org/10.1021/es304940s
32. Xu D, Yang L, Wang Y et al (2018) Proteins enriched in charged amino acids control the formation and stabilization of selenium nanoparticles in Comamonas testosteroni S44. Sci Rep 8:1–11. https://doi.org/10.1038/s41598-018-23295-5

33. Misra SK, Dybowska A, Berhanu D et al (2012) The complexity of nanoparticle dissolution and its importance in nanotoxicological studies. Sci Total Environ 438:225–232. https://doi.org/10.1016/j.scitotenv.2012.08.066
34. Selmani A, Seibert E, Tetyczka C et al (2022) Thiolated Chitosan Conjugated Liposomes for Oral Delivery of Selenium Nanoparticles. Pharmaceutics 14. https://doi.org/10.3390/pharmaceutics14040803
35. Bai K, Hong B, Hong Z et al (2017) Selenium nanoparticles-loaded chitosan/citrate complex and its protection against oxidative stress in d-galactose-induced aging mice. J Nanobiotechnol 15. https://doi.org/10.1186/s12951-017-0324-z
36. Xia Y, Zhao M, Chen Y et al (2018) Folate-targeted selenium nanoparticles deliver therapeutic siRNA to improve hepatocellular carcinoma therapy. RSC Adv 8:25932–25940. https://doi.org/10.1039/c8ra04204g
37. Li HF, McGrath SP, Zhao FJ (2008) Selenium uptake, translocation and speciation in wheat supplied with selenate or selenite. New Phytol 178:92–102. https://doi.org/10.1111/j.1469-8137.2007.02343.x
38. Khan MS, Soyk A, Wolf I et al (2022) Discriminative Long-Distance Transport of Selenate and Selenite Triggers Glutathione Oxidation in Specific Subcellular Compartments of Root and Shoot Cells in Arabidopsis. Front Plant Sci 13. https://doi.org/10.3389/fpls.2022.894479
39. Eiche E, Bardelli F, Nothstein AK et al (2015) Selenium distribution and speciation in plant parts of wheat (Triticum aestivum) and Indian mustard (Brassica juncea) from a seleniferous area of Punjab, India. Sci Total Environ 505:952–961. https://doi.org/10.1016/j.scitotenv.2014.10.080
40. Wang K, Wang Y, Li K et al (2020) Uptake, translocation and biotransformation of selenium nanoparticles in rice seedlings (Oryza sativa L). J Nanobiotechnol 18. https://doi.org/10.1186/s12951-020-00659-6
41. Yang X, Xu H, Li W et al (2025) Effects of Nanomaterials on Crops. Curr Issues Mol Biol 47:1024. https://doi.org/10.3390/cimb47121024
42. Yang C, Wang C, Khan Z et al (2023) Algal polysaccharides–Selenium nanoparticles regulate the uptake and distribution of selenium in rice plants. Front Plant Sci 14. https://doi.org/10.3389/fpls.2023.1135080
43. Soni S, Singh KM, Jha AB et al (2026) Size-based dynamics of nanoparticles in plant growth and environmental stress tolerance: potential benefits and hazards. Environ Sci Nano 13:58–78
44. Lv J, Christie P, Zhang S (2019) Uptake, translocation, and transformation of metal-based nanoparticles in plants: recent advances and methodological challenges. Environ Sci Nano 6:41–59
45. Van Der Ent A, Salinitro M, Brueckner D et al (2023) Differences and similarities in selenium biopathways in Astragalus, Neptunia (Fabaceae) and Stanleya (Brassicaceae) hyperaccumulators. Ann Bot 132:349–361. https://doi.org/10.1093/aob/mcad110
46. Li Y, Zhu N, Liang X et al (2020) A comparative study on the accumulation, translocation and transformation of selenite, selenate, and SeNPs in a hydroponic-plant system. Ecotoxicol Environ

Saf 189. https://doi.org/10.1016/j.ecoenv.2019.109955

47. Montanari S, Salinitro M, Simoni A et al (2023) Foraging for selenium: a comparison between hyperaccumulator and non-accumulator plant species. Sci Rep 13. https://doi.org/10.1038/s41598-023-37249-z
48. Galić L, Vinković T, Ravnjak B, Lončarić Z (2021) Agronomic biofortification of significant cereal crops with selenium—a review. https://doi.org/10.3390/agronomy11051015. Agronomy 11:
49. Ramkissoon C, Degryse F, da Silva RC et al (2019) Improving the efficacy of selenium fertilizers for wheat biofortification. Sci Rep 9. https://doi.org/10.1038/s41598-019-55914-0
50. Siddiqui SA, Blinov AV, Serov AV et al (2021) Effect of selenium nanoparticles on germination of hordéum vulgáre barley seeds. Coatings 11. https://doi.org/10.3390/coatings11070862
51. Ikram M, Raja NI, Javed B et al (2020) Foliar applications of bio-fabricated selenium nanoparticles to improve the growth of wheat plants under drought stress. Green Process Synth 9:706–714. https://doi.org/10.1515/gps-2020-0067
52. Badawy SA, Zayed BA, Bassiouni SMA et al (2021) Influence of nano silicon and nano selenium on root characters, growth, ion selectivity, yield, and yield components of rice (Oryza sativa l.) under salinity conditions. Plants 10. https://doi.org/10.3390/plants10081657
53. Jain R, Gonzale-Gil G, Singh V et al (2014) Biogenic Selenium Nanoparticles: Production, Characterization and Challenges. In: Biotechnology Volume 10: Nanobiotechnology. pp 365–394
54. Mal J, Veneman WJ, Nancharaiah YV et al (2017) A comparison of fate and toxicity of selenite, biogenically, and chemically synthesized selenium nanoparticles to zebrafish (Danio rerio) embryogenesis. Nanotoxicology 11:87–97. https://doi.org/10.1080/17435390.2016.1275866
55. Ohlendorf HM, Hoffman DJ, Saiki MK, Aldrich TW (1986) Embryonic mortality and abnormalities of aquatic birds: Apparent impacts of selenium from irrigation drainwater. Sci Total Environ 52:49–63. https://doi.org/10.1016/0048-9697(86)90104-X
56. Lemly AD, Skorupa JP (2012) Wildlife and the coal waste policy debate: Proposed rules for coal waste disposal ignore lessons from 45 years of wildlife poisoning. Environ Sci Technol 46:8595–8600. https://doi.org/10.1021/es301467q
57. Henry BL, Wesner JS, Kerby JL (2020) Cross-Ecosystem Effects of Agricultural Tile Drainage, Surface Runoff, and Selenium in the Prairie Pothole Region. Wetlands 40:527–538. https://doi.org/10.1007/s13157-019-01194-3
58. Zhang T, Qi M, Wu Q et al (2023) Recent research progress on the synthesis and biological effects of selenium nanoparticles. Front Nutr 10

Figures

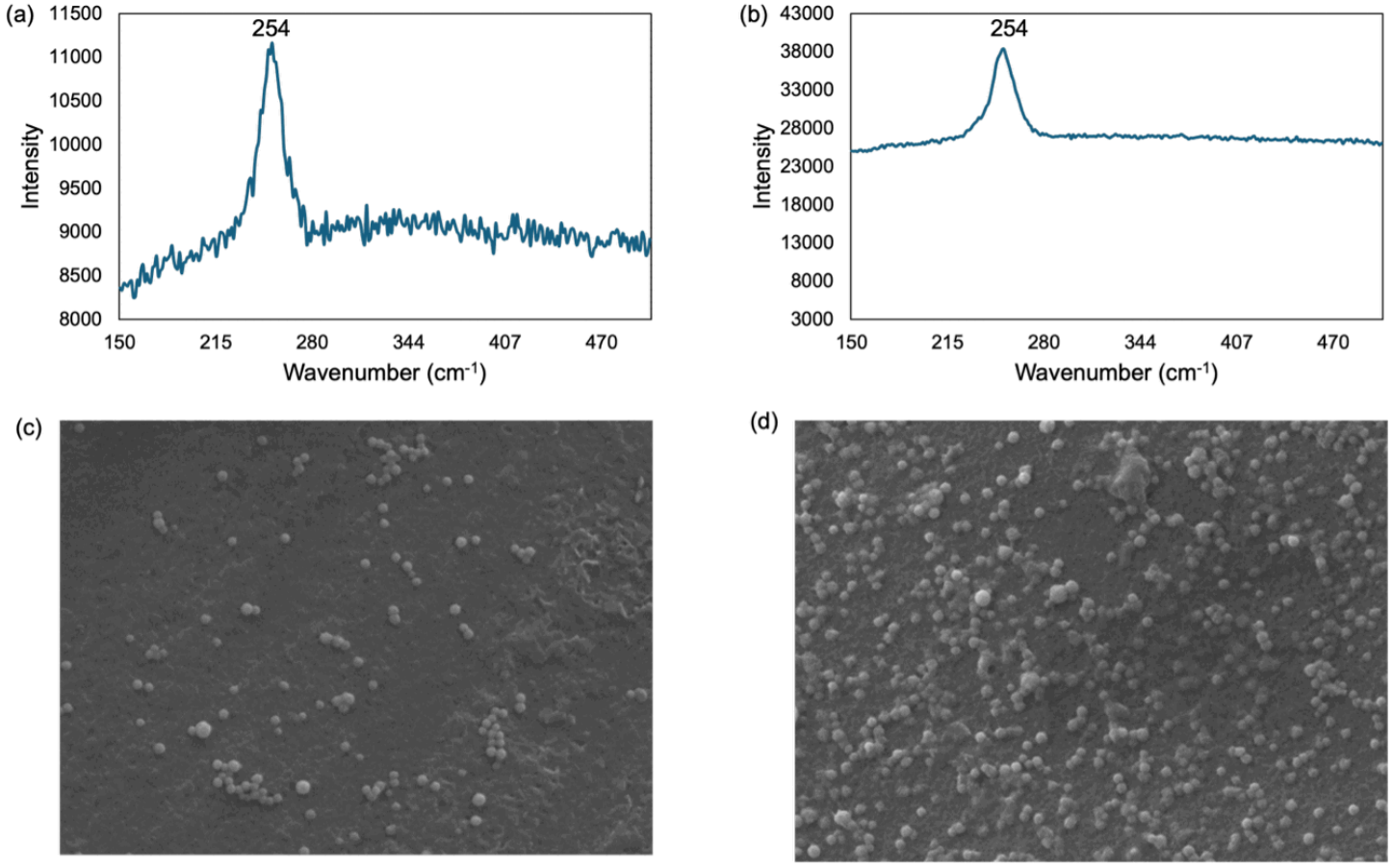


Figure 1

Raman spectra for BioSeNPs produced by (a) *E. coli* and (b) Anaerobic granular sludge. SEM images of BioSeNPs produced by (c) *E. coli* and (d) Anaerobic granular sludge.

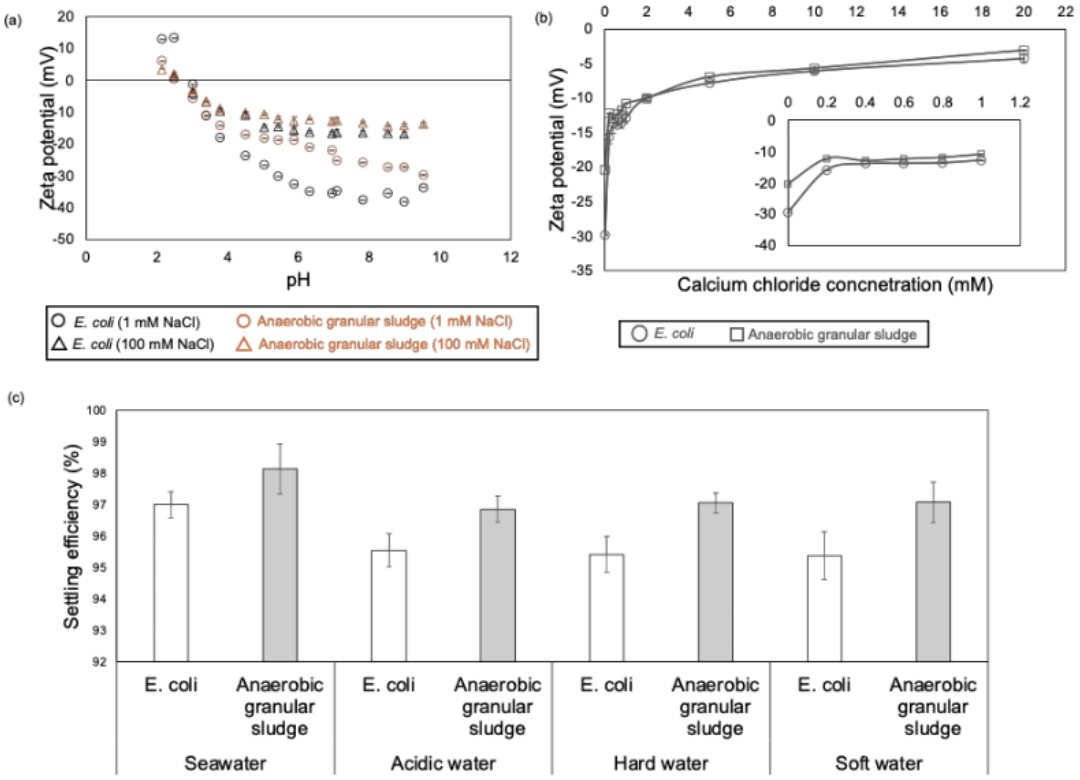


Fig 2. (a) Zeta potential variation of BioSeNPs with respect to pH at varied concentration of the background electrolyte (NaCl). Black circles (○) and orange circles (○) represent BioSeNPs produced by *E. coli* and anaerobic granular sludge in 1 mmol·L^{-1} NaCl, respectively. Black triangles (Δ) and orange triangles (Δ) represent BioSeNPs produced by *E. coli* and anaerobic granular sludge in 100 mmol·L^{-1} NaCl, respectively. (b) Zeta potential trend of BioSeNPs produced by *E. coli* (○) and the anaerobic granular sludge (□) on addition of calcium chloride over the range of 0-20 mmol·L^{-1} (c) Settling efficiency of BioSeNPs in seawater, acidic water and freshwater (hard and soft).

Figure 2

See image above for figure legend

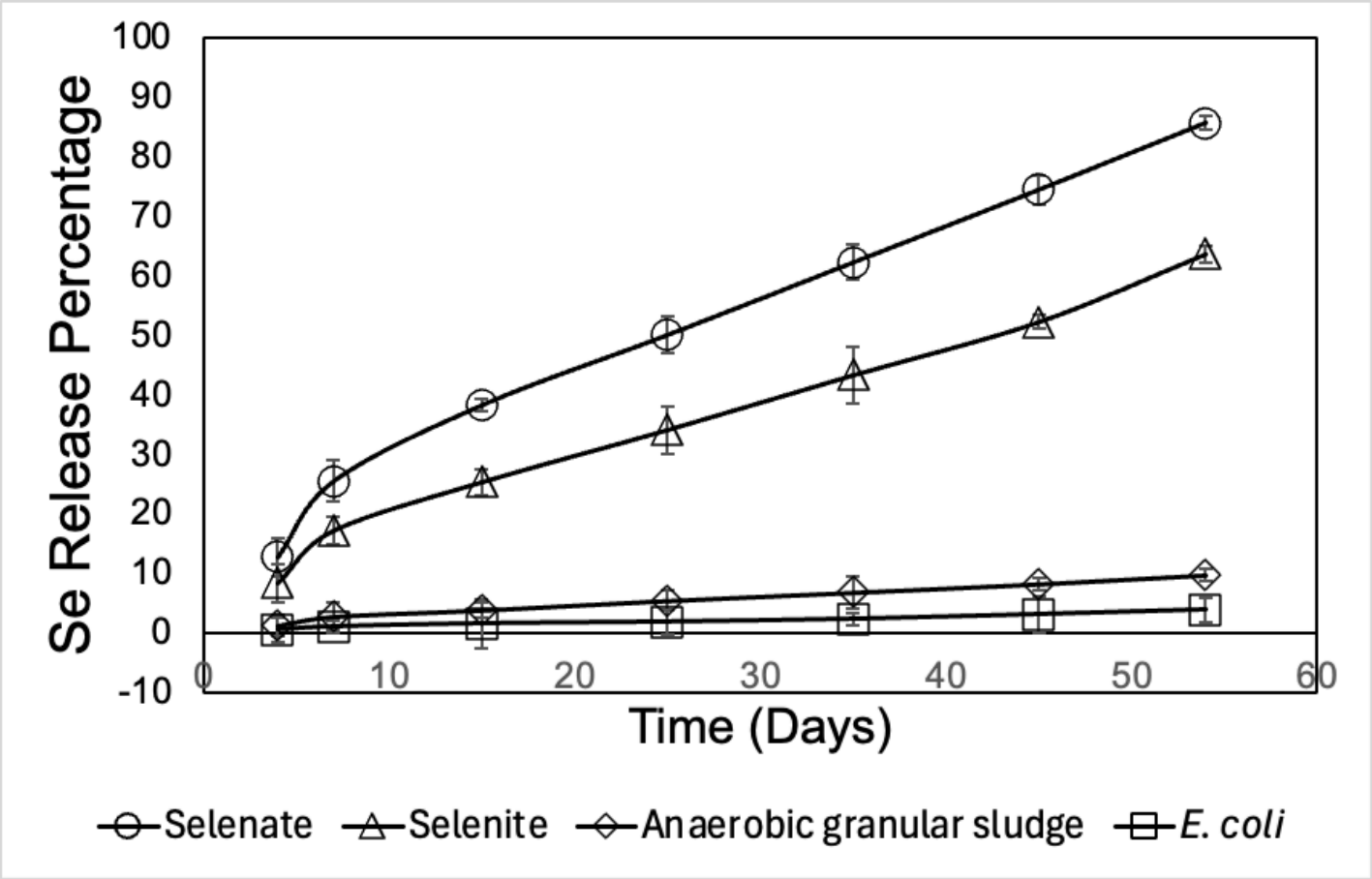


Fig 3. Percentage of Se released and lost in water as leachate from the soil on watering the soil has been shown for 8 weeks. Selenate, selenite and BioSeNPs produced by anaerobic granular sludge and *E. coli* are represented by circle (○), triangle (Δ), rhombus (◊) and square (□), respectively.

Figure 3

See image above for figure legend

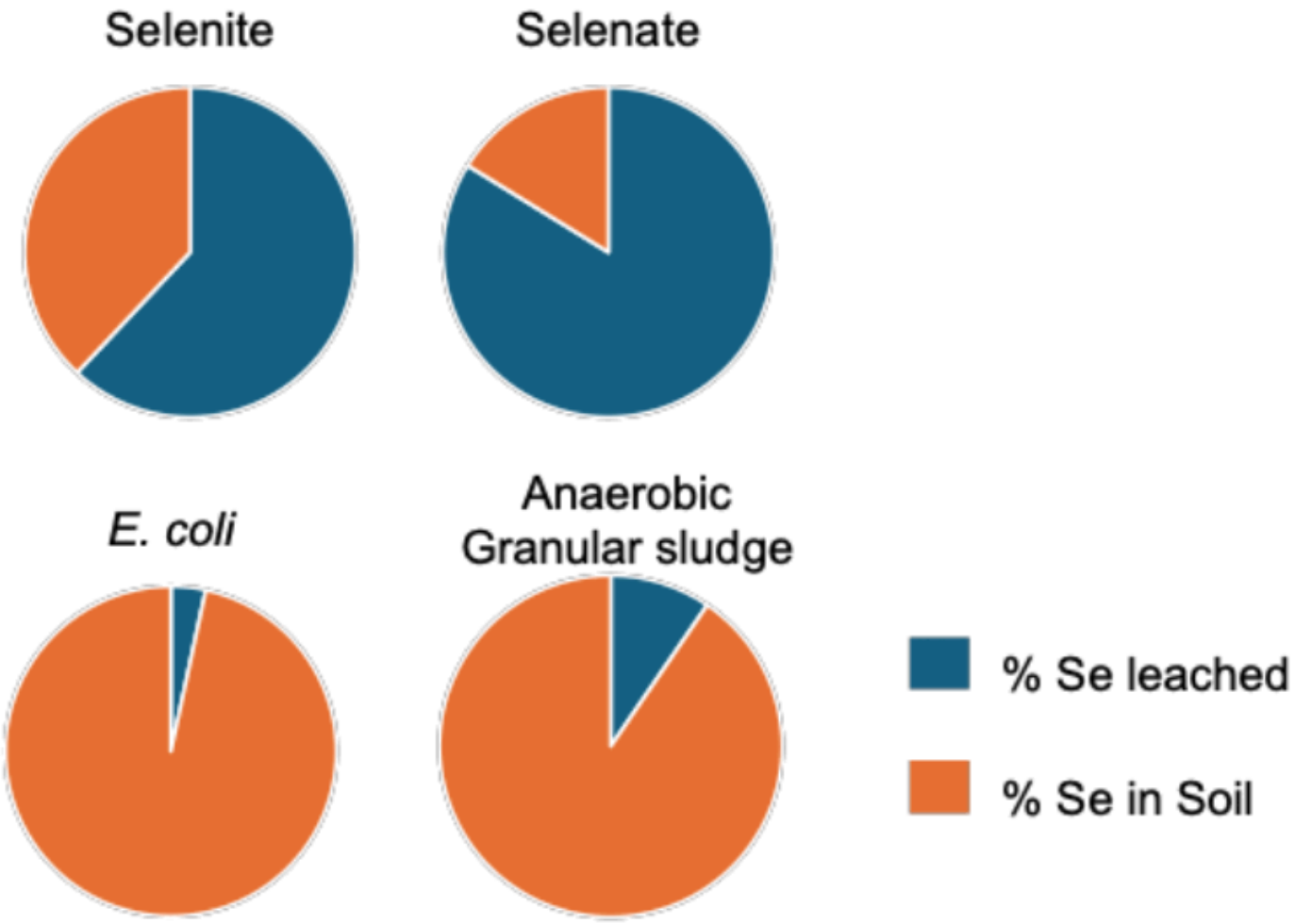


Figure 4

The amount of Se retained in soil and lost as leachate by the end of 8 weeks has been represented in the form of a pie chart. Orange represents the amount of Se in soil, and blue represents the amount of Se leached out in water.

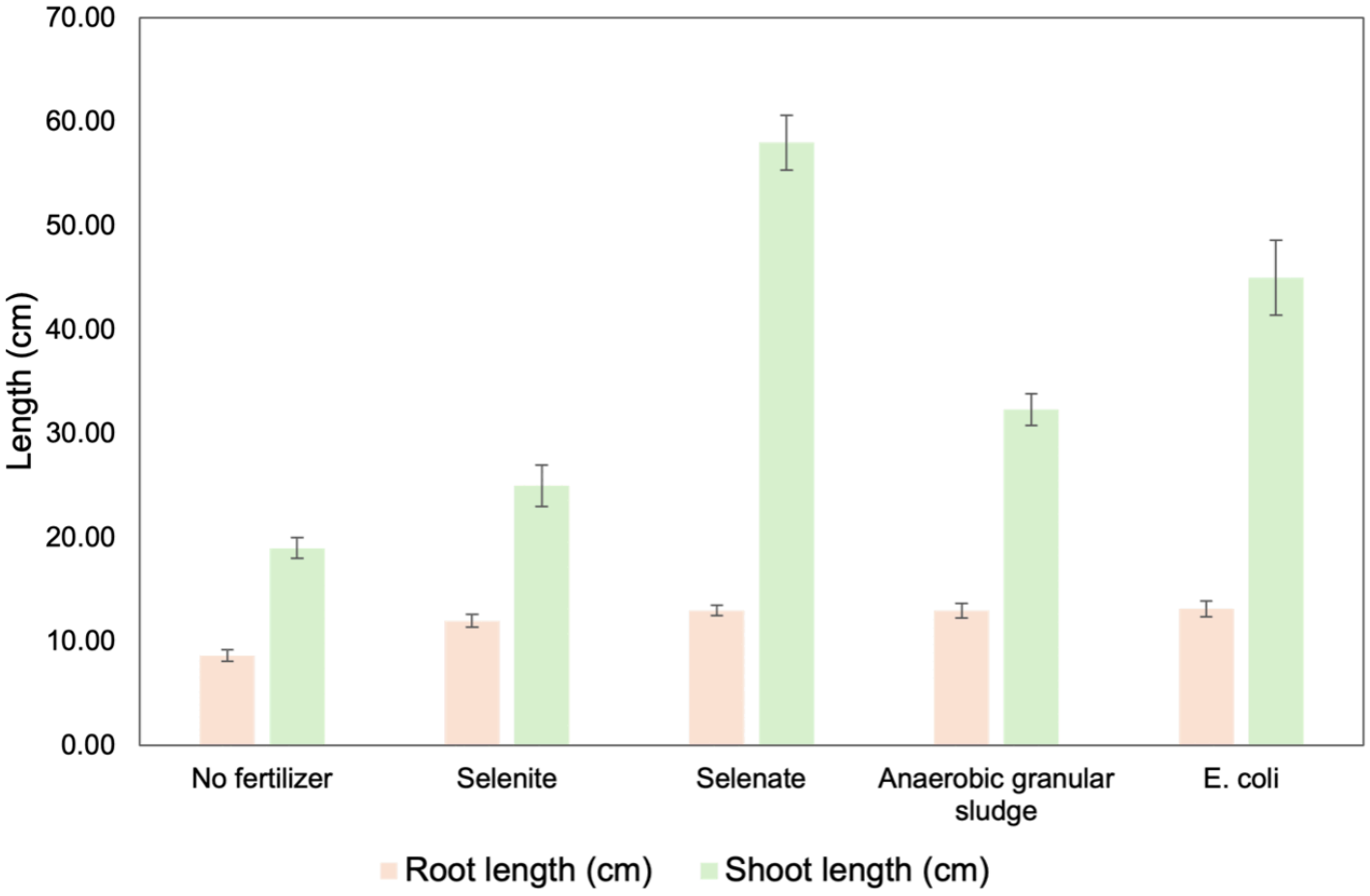


Figure 5

The average root and shoot length of plants with or without Se fertilization has been represented in cm in the bar charts at Day 56. Root length is shown in orange, whereas shoot length is represented by green columns.

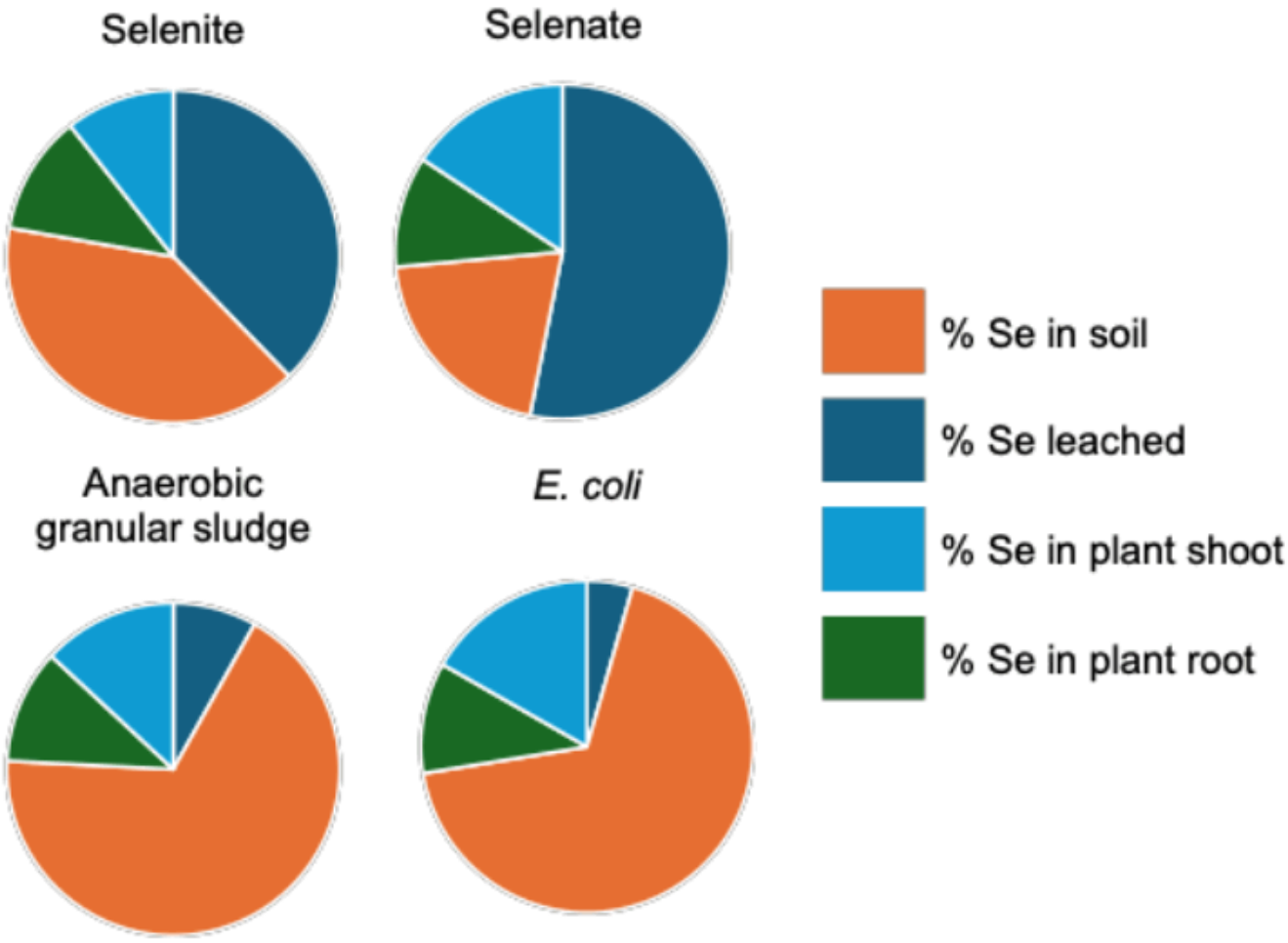


Figure 6

The distribution of Se in plants, soil and leachate has been mapped in the form of a pie chart for all types of Se fertilization done in this study at Day 56. Dark blue represents the amount of Se leached from the soil, orange, light blue and green represent the amount of Se in soil, shoots and roots, respectively.

Supplementary Files

This is a list of supplementary files associated with this preprint. Click to download.

- SeslowreleasefertilizerSI.docx
- floatimage1.png